John von Neumann Institute for Computing

Meson Form Factors

Jan van der Heide, Justus Koch, Edwin Laermann

published in

NIC Symposium 2004, Proceedings,
Dietrich Wolf, Gernot Münster, Manfred Kremer (Editors),
John von Neumann Institute for Computing, Jülich,
NIC Series, Vol. **20**, ISBN 3-00-012372-5, pp. 129-138, 2003.

http://www.fz-juelich.de/nic-series/volume20

Meson Form Factors

Jan van der Heide[1], **Justus Koch**[1], **and Edwin Laermann**[2]

[1] National Institute for Nuclear Physics and High Energy Physics (NIKHEF)
1009 DB Amsterdam, The Netherlands
E-mail: {r86, justus}@nikhef.nl

[2] Fakultät für Physik, Universität Bielefeld
33615 Bielefeld, Germany
E-mail: edwin@physik.uni-bielefeld.de

We calculate the electromagnetic form factor of the pion in lattice gauge theory. The non-perturbatively improved Sheikoleslami-Wohlert lattice action is used together with the $\mathcal{O}(a)$ improved current. The form factor is compared to results for another choice for the current and features of the structure of the pion deduced from the 'Bethe-Salpeter amplitude' are discussed. Prospects for the case of non-vanishing temperature are briefly commented on.

1 Introduction

For the matter surrounding us we are used to the fact that it can be broken down into its building blocks. This is true for molecules, atoms and nuclei. However, for nucleons, the building blocks of nuclei, and other elementary particles subject to the strong interaction that *e.g.* binds nucleons into a nucleus, this is not possible anymore. Quantum chromodynamics (QCD), the fundamental theory of the strong interaction, is based on quarks and gluons as the degrees of freedom that describe the internal structure and dynamics of hadrons. The forces between these constituents become extremly strong for separations on the order if the radius of a hadron, typically $1\ \mathrm{fm} = 10^{-13}\ \mathrm{cm}$. Therefore no free quark or gluon has ever been observed, they can only live locked up inside hadrons. This highly unusual and very intriguing aspect of QCD is referred to as 'confinement'.

To date it has been impossible to find analytical solutions for the structure of hadrons in the context of QCD. Due to the strength of the interaction, also perturbative methods cannot be applied. A variety of effective 'QCD inspired' models exist, but the salient QCD feature of confinement is put in by hand. The only way to work within QCD without model assumptions and to arrive at confinement from first priciples has been lattice QCD, a method which this project uses.

Rather than calculating a global property, such as hadron masses, within lattice QCD, we aim in this project at details of the intrinsic structure of the pion, the lightest hadron. In its simplest description, the pion is a bound quark - antiquark system. The observable we focus on is the electric form factor, a directly measurable quantity which essentially corresponds to the Fourier transform of the charge distribution of the pion. The only building blocks in QCD that do carry electric charge are the pointlike quarks.

The pion as the simplest particle with only two valence quarks has been the subject of many studies. Global features of the pions - their charge and spin - are easily incorporated in model calculations. The form factor, which directly reflects the internal structure of this elementary particle, is clearly an important challenge. Many earlier calculations are based on *ad hoc* models that model QCD or sum over selected subsets of Feynman diagrams.

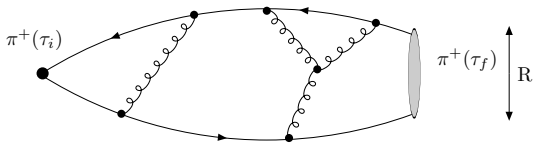

Figure 1. Two-point function.

However, the most reliable approach, in particular when addressing non-perturbative features as the electromagnetic form factor at intermediate momentum transfers, is the use of lattice QCD. First lattice results were obtained by Martinelli and Sachrajda[1], which was followed by a more detailed study by Draper *et al.*[2], who showed that the form factor obtained through lattice QCD with the Wilson action could be described by a simple monopole form as suggested by vector meson dominance[3]. We extended[4] these early studies in two ways. We use an improved lattice action[5,6] and a consistently improved electromagnetic current operator[7–9]. Furthermore, we also extend the calculations to lower pion masses than achieved before. Several features of the internal structure of the pion have been obtained previously[10–14] by calculating the 'Bethe-Salpeter amplitude', which can be used to estimate the relative separation of the quark-antiquark pair in the pion and thus its charge radius. We also use this approach and compare its predictions to the results of our direct calculation of the pion form factor.

2 The Method

In solving QCD by lattice methods, one replaces the continuous space and time coordinates by a grid of discrete points. This step clearly implies a numerical error which one has to control. In our calculation, we have chosen an approach that describes the dynamics of quarks and gluons in terms of the so-called 'improved action'. It guarantees that there are no errors to first order in the lattice spacing a, a major difference to earlier attempts to obtain the pion form factor.

It is well known that lattice methods do not immediately yield the physical properties of hadrons one is interested in, but require extrapolation of the results. For example, the calculated pion mass is much higher than the observed mass of 140 MeV. In the earlier form factor calculations, the mass was on the order of 1000 MeV. In our calculation, we work with pion masses from 1 GeV down to 360 MeV, which allows us to extrapolate our results towards the physical limit.

In common with earlier work (and with at present the majority of lattice calculations), we work in the 'quenched approximation'. It includes the propagation in space and time of the quark and antiquark in the pion. The creation of additional pairs, which QCD allows in principle, is not included. The gluons, on the other hand, are taken into account with their full dynamics and without any restrictions.

In order to arrive at the quantity of interest, the pion form factor, we consider two situations of a propagating quark - antiquark pair, a two- and three-point function. The propagation is considered in normal three-dimensional space, but in imaginary time τ, *i.e.* one substitutes $t \rightarrow -i\tau$.

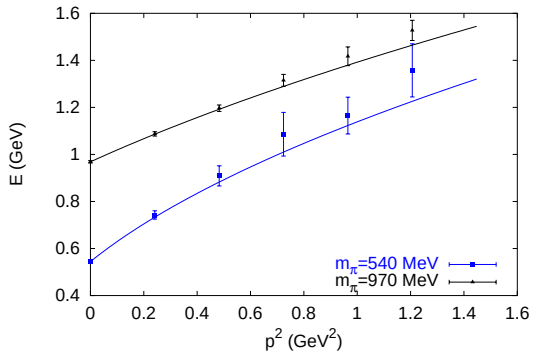

Figure 2. The energy momentum relation $E_{\mathbf{p}} = E(\mathbf{p})$. The data for two different pion masses at various (discrete) lattice momenta are compared to the continuum prediction.

In the two point function G_2 (see Fig. 1), a quark - antiquark pair is created at an initial space-time point $\{\vec{x}_i, \tau_i\}$. Using the dynamics contained in the discretized improved QCD action, one then propagates the pair in space and (imaginary) time to a final point $\{\vec{x}_f, \tau_f\}$. As the quark pair travels along, arbitrarily many and complex interactions between them by means of gluon exchanges are taken into account in lattice QCD. Due to the fact that the time is purely imaginary, the propagation is damped according to $e^{-\mathcal{H}\tau}$, where $\mathcal{H}$ is the Hamiltonian. For sufficiently large propagation time $\tau = \tau_f - \tau_i$, this filters out the state with the lowest energy of the quark - antiquark system. For the quarks we chose, an 'up' and anti - 'down' quark, this lowest state is a π^+ meson. By determining its energy from the exponential fall-off in τ and Fourier - projecting onto various three-momentum states, we can determine the mass of the pion. Fig. 2 shows the obtained energy E as a function of several projected momenta $\vec{p}$. Comparison with the usual connection between energy and momentum (lines) shows that we are for the relevant momenta in our study ($p^2 \leq 0.5$ GeV^2) very close to the continuum situation.

As we are interested in the ground state of the pion, we can enhance the probability of the quark-antiquark pair to arrive at the point $\{\vec{x}_f, \tau_f\}$ as a pion. Instead of letting the quarks come together again at one point, we instead let them be separated by a distance R as indicated in Fig. 1. Due the finite size of the pion, one is more likely to find the two quarks at a finite separation. This technique[13] to improve the contribution from the ground state is referred to as 'smearing'. In fact, by varying the distance R, one can map out the probability amplitude $\Phi(R)$ for quarks to have a given separation. This amplitude is commonly referred to as the 'Bethe Salpeter amplitude'. It will be discussed below to what extent this amplitude can provide information about the charge distribution and thus the form factor of a pion.

The three-point function G_3, shown in Fig. 3, directly involves the quantity of interest, the electromagnetic form factor. This form factor is part of the photon - pion vertex. In order to obtain this vertex in lattice QCD, one again propagates a quark - antiquark pair long enough to filter out the pion. At an intermediate time τ, a photon is then coupled two either one of the two charged quarks and the resulting state is again propagated long enough that only the ground state survives. In order to arrive at the situation for a given

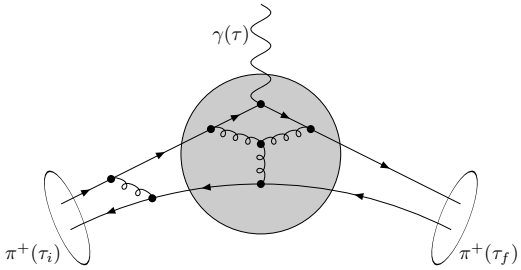

Figure 3. Three-point function.

three-momentum transfer, we project onto specific initial and final pion three-momenta, $\mathbf{p}_i$ and $\mathbf{p}_f$ to obtain $G_3(\tau_f, \tau, \tau_i; \mathbf{p}_f, \mathbf{p}_i)$

When calculating this three-point function, it is important to use the quark current operator that is consistent with the improved action. In the continuum case, the current of a quark has the general form

$$j_\mu^L = \bar{\psi}(x)\gamma_\mu\psi(x). \tag{1}$$

A conserved Noether current j_μ^C can also be derived on the lattice, *i.e.* at finite lattice spacing. This current does not need to be renormalized as it is conserved, but receives $\mathcal{O}(a)$ corrections at non-vanishing momentum transfer between the pions, $\vec{q} = \vec{p}_f - \vec{p}_i \neq 0$. It is, however, possible to define an 'improved conserved current' which is of the form[7–9]

$$j_\mu^I = Z_V \left\{ j_\mu^L + a\, c_V\, \partial_\nu\, T_{\mu\nu} \right\} . \tag{2}$$

It contains, in addition to the normal continuum current, a tensor operator

$$T_{\mu\nu} = \bar{\psi}(x)\; i\; \sigma_{\mu\nu}\; \psi(x) \tag{3}$$

and a renormalization factor Z_V

$$Z_V = Z_V^0\; (1 + a\, b_V\, m_q) \; . \tag{4}$$

The coefficients Z_V^0, b_V and C_V in j_μ^I can be determined such that the matrix elements of the current receive no corrections to $\mathcal{O}(a)$. The difference between the 'improved conserved current' and the 'conserved current' will further be illustrated below.

3 Details of the Calculation

In our calculation, we work with a grid consisting of $N_\sigma = 24$ points in each spatial and $N_\tau = 32$ points in the time direction. The separation a of these points is chosen equal in space and time. As in Ref. 15, we take $a = 0.105\ \mathrm{fm}$, corresponding to a spatial extension of $N_\sigma\, a = 2.5\,\mathrm{fm}$. This is sufficient for computing the structure of the pion, which has a radius of about $0.7\mathrm{fm}$. Each of the $24^3 \times 32$ lattice points carries in addition labels for the internal quantum numbers for quarks and gluons. This greatly increases the dimensionality of the problem and makes the use of supercomputers absolutely essential.

An important task is the generation of a set of representative gluon configurations on this multi-dimensional grid. We work with a set of 100 configurations for the so called gluon link variables at a coupling of $6/g^2 = 6$. After an initial thermalisation of 2500 sweeps, we obtained configurations at intervals of 500 sweeps. Each sweep consists of a pseudo-heatbath step with FHKP updating in the $SU(2)$ subgroups, followed by four over-relaxation steps. In contrast to the Dirichlet conditions in Ref. 2, where the fields are assumed to vanish on the lattice boundaries, we imposed anti-periodic boundary conditions on the quarks and periodic boundary conditions on the gluons.

The most time consuming part, in particular for light quarks, consists of the calculation of quark propagators. In the part of the action specifying the quark dynamics, the choice of the 'hopping parameter' κ determines the quark and also the pion mass. Our choices correspond to

$$m_\pi = 970,\ \ 780,\ \ 670,\ \ 540,\ \ \text{and}\ \ 360\,\text{MeV}\ . \tag{5}$$

We utilized an improved action[5] with a non-perturbative[6] value of $c_{SW} = 1.769$ for the improvement operator. For the improved current, we also use the non-perturbatively determined[16] values of the parameters Z_V^0, b_V and c_V.

As the calculations are very lengthy and involved, it is important to have an independent test. Conservation of the total charge generated at the source at τ_i provides a test[2] for our calculation, relating the $\mu = 4$ component of the three-point function for $\mathbf{q} = 0$ to the two-point function. For our periodic boundary conditions, this test connects the independently determined two- and three-point functions,

$$G_3(\tau_f, \tau, \tau_i; \mathbf{p}, \mathbf{p}) - G_3(\tau_f, \tau', \tau_i; \mathbf{p}, \mathbf{p}) = G_2(\tau_f - \tau_i, \mathbf{p})\ , \tag{6}$$

where $\tau_f < \tau' < N_\tau$. We find that all configurations we use each satisfy this condition to at least 1 ppm.

For the results discussed below, we chose the pion three-momenta in the three-point function such that $|\mathbf{p}_i|^2 = |\mathbf{p}_f|^2 = 2$ in units of the minimum momentum $\frac{2\,\pi}{a\,N_\sigma}$ for our lattice. This guarantees for the elastic pion form factor that $E_f - E_i = q_0 = 0$ and greatly simplifies the kinematic factors appearing in the three-point function. Different three-momentum transfers $\mathbf{q}$ were obtained by varying the relative orientation of the initial and final pion momenta.

As already discussed, to improve the projection onto the ground state, we smeared the pion operator at the sink τ_f in G_2 and G_3 by the method proposed in Ref. 13. We found that a quark-antiquark distance $R = 3$ works best. The quark-antiquark pair was connected by APE smeared gluon links at smearing level 4 and relative weight 2 between straight links and staples.

From the numerical lattice results for the two- and three-point functions the desired information is extracted by fits. For the two-point function with the pion propagating in its ground state, we use the form

$$G_2(\tau, \mathbf{p}) = \sqrt{Z_R^\pi(\mathbf{p}) Z_0^\pi(\mathbf{p})}\ e^{-\,E_{\mathbf{p}}^\pi\ \frac{N_\tau}{2}}\ \cosh\{E_{\mathbf{p}}^\pi\,(\frac{N_\tau}{2} - \tau)\}\ , \tag{7}$$

where the $\cosh$-form reflects the periodic boundary conditions and the Z-factors are related to the Bethe-Salpeter amplitude,

$$\Phi(R) = \sqrt{Z_R^\pi(\mathbf{0})\ /\ Z_0^\pi(\mathbf{0})}\ . \tag{8}$$

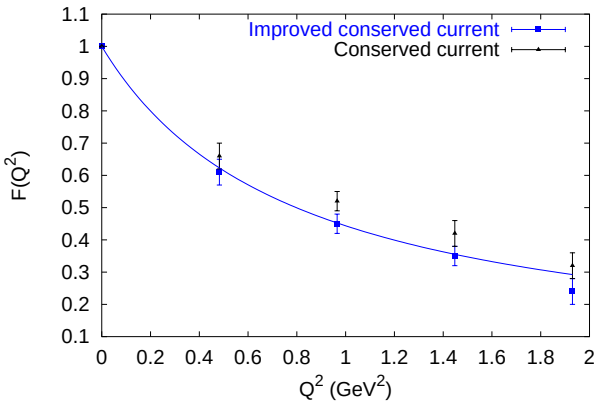

Figure 4. Form factors for the conserved and improved current at the second lowest pion mass, $m_\pi = 540$ MeV. The solid line is the monopole form, Eq. 11, with m_ρ taken from literature (see text).

A similar term for a first excited state is also included.

General considerations show that the matrix elements of the electromagnetic current between free pions must have the form

$$\langle \pi(\mathbf{p}_f)|j_\mu|\pi(\mathbf{p}_i)\rangle = (p_f + p_i)_\mu \; F(Q^2) \; , \tag{9}$$

where $F(Q^2)$ is the pion form factor and $Q^2 = -(p_f - p_i)^2 > 0$. Choosing $\mu = 0$ the three-point function can be parametrised as

$$G_3(\tau_f, \tau, \tau_i; \mathbf{p}_f, \mathbf{p}_i) = F(Q^2) \sqrt{Z_R^\pi(\mathbf{p}_f) \; Z_\pi^0(\mathbf{p}_i)} e^{-E^\pi_{\mathbf{p}_f} \; (\tau_f - \tau) - E^\pi_{\mathbf{p}_i} \; (\tau - \tau_i)} \; . \tag{10}$$

Terms that take a transition to the first excited state into account are also included. Effects involving, for example, the production of pion pairs, as well as 'wrap around effects' due to the propagation of states beyond N_τ are exponentially suppressed ($< \mathcal{O}(e^{-5})$); similarly, an elastic contribution from the excited state was estimated to be of the order of 1% or less. All these effects are not reflected in our chosen parametrisation.

All parameters in the 2- and 3-point functions - energies E, Z-factors and the form factor $F(Q^2)$ - were fit simultaneously to the data from all configurations. For the three-point function, we chose $\tau_f = 11$ and let the current insertion time τ vary from 0 to 10. For maximum spatial symmetry, all values corresponding to the same value $|\mathbf{p}|$ in the two-point function and all $\mathbf{p}_{i,f}$ yielding the same $\mathbf{q}$ in the three-point function were combined for the fit. The values for the parameters and their errors in these simultaneous fits were obtained through a single elimination jackknife procedure. Since we satisfy Eq. 6 to high accuracy, we show $F(0) = 1$ in the results below instead of using the result from a fit at $Q^2 = 0$, which would be less accurate in this case.

4 Results

As mentioned in the previous section, our method to extract the pion form factor is non-perturbatively improved in two respects: we use an improved action and an improved

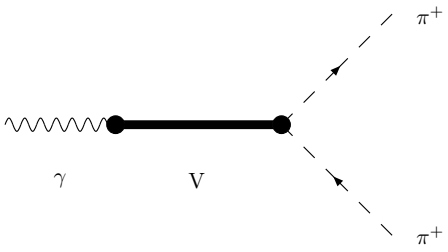

Figure 5. VMD model.

current operator. One can get an impression of the importance of the latter step by comparing the conserved Noether current corresponding to the improved action with the improved current (which is also conserved). The results [a] are shown in Fig. 4 for the second lightest of the five pion masses we have analyzed. The form factor from the improved current is systematically lower than the one from the conserved current. The difference grows with Q^2 and reaches about 25% at the largest momentum transfer considered here.

It is worth mentioning that with the Z_V, c_V and b_V values taken from Ref. 16, and performing a fit at $Q^2 = 0$ we obtained $F^I/F^C = 1$ to better than 1% with a statistical error of about 5%.

The results can be described by a monopole form factor

$$F(Q^2) = \{1 + \frac{Q^2}{m_V^2}\}^{-1} \,, \tag{11}$$

a form suggested by vector meson dominance (VMD). In this model the pion-photon coupling is dominated by the exchange of a vector meson V to which photon as well as the pions can couple, see Fig. 5. The prime candidate is the lightest vector meson in the QCD spectrum, the ρ. In fact, in Fig. 4 we also show a monopole form factor using the value for the ρ-mass obtained by interpolating the lattice results from Ref. 17 which uses the same action as we do. This monopole form describes our results for the improved current at all but the highest Q^2 very well. We observe that the conserved current lies consistently above the monopole form factor. A similar behaviour was found also for our other κ-values.

In Fig. 6 we show our results for improved form factors for all five values for the pion mass. The form factors systematically decrease with decreasing pion mass. The statistical error of the extracted form factors grows as the quark mass decreases. Nevertheless, we still obtain conclusive results for the smallest quark mass. The corresponding pion mass of 360 MeV is substantially lower than in the previous work, where $m_\pi \simeq 1$ GeV.

We also fitted our results for the improved form factors to a monopole form factor. In doing so, we omitted the highest momentum data point and extracted in each case a vector meson mass, m_V. It turns out that the fit results for m_V are close, with deviations of at most 5 %, to the values for m_ρ taken from interpolations to literature data[17].

The form factor allows to extract the mean-square charge radius $\langle r^2 \rangle$ from its low-Q^2

[a] In all our results we only show the statistical errors.

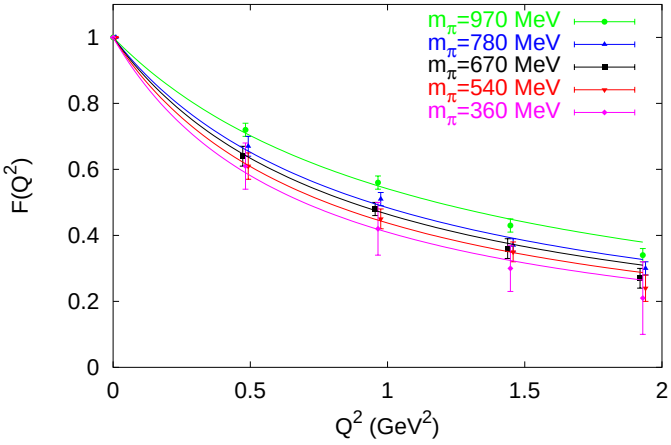

Figure 6. Form factors as a function of Q^2 for the five pion masses. Curves are monopole fits to the data with one free parameter, the vector meson mass m_V, see Eq. 11.

behaviour according to

$$\left.\frac{dF(Q^2)}{dQ^2}\right|_{Q^2=0} = -\frac{1}{6}\left\langle r^2\right\rangle_{FF} \ . \tag{12}$$

The results are shown in Fig. 7 as a function of the pion mass. As can be seen, the radius shows a substantial dependence on the mass.

Previously, the 'Bethe-Salpeter-amplitude' $\Phi(R)$ has been used to obtain estimates of the charge radius,

$$\left\langle r^2\right\rangle_{BS} := \frac{1}{4}\frac{\int d^3\vec{r}\,\vec{r}^{\,2}\ \Phi^2(|\vec{r}|)}{\int d^3\vec{r}\,\Phi^2(|\vec{r}|)\ .} \tag{13}$$

The results based on this procedure are shown in Fig. 7 as a function of the pion mass. First of all, the values are much lower than the results originating from the form factor. Furthermore, in agreement with the findings of Refs. 10–12, 14, we see that the Bethe-Salpeter predictions are very insensitive to the value of the quark or pion mass. However, it is well known[12] that the information that can be obtained from the Bethe-Salpeter approach as described above is only an approximation. It assumes, in the extraction of $\left\langle r^2\right\rangle$, that the center of mass of the pion is always halfway between the valence quark and antiquark, not allowing for the motion of the gluons. Our form factors and the charge radii extracted from them, on the other hand, do not involve this restriction on the valence (anti-)quark motion. The comparison of the results in Fig. 7 for the first time shows the size of this assumption inherent to the Bethe-Salpeter approach. The quark or pion mass dependence of this effect demonstrates that the lighter the quark masses, the more the motion of the center-of-mass is affected by the gluon energy in the pion.

In order to describe the data on the form factor or the charge radii as a function of the pion mass one could attempt to use predictions of chiral perturbation theory. Chiral perturbation theory (χPT) is an effective field theory approach built on a systematic expansion

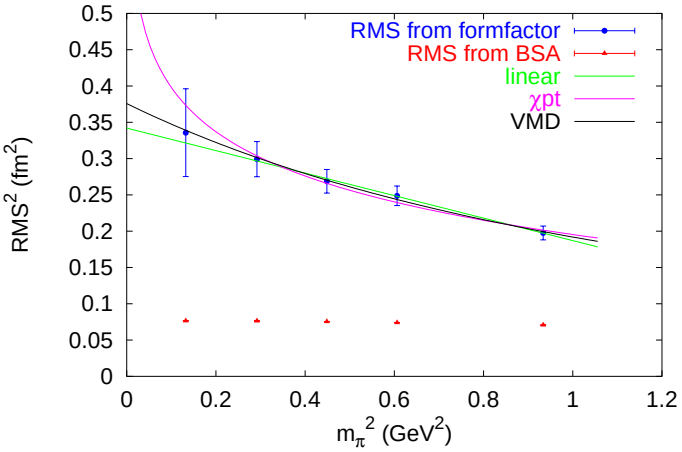

Figure 7. Radii of the pion as obtained from Bethe-Salpeter amplitudes (BSA), Eq. 13, and from the form factors, Eq. 12. Also shown are three different parametrizations of $\langle r^2 \rangle$ as function of m_π^2 (see text): (χPT) inspired form, Eq. 14, contributions expected to dominate in qχPT and VMD ansatz.

around the chiral limit at which the pion mass vanishes. It thus has the potential to bridge the gap between the physical limit, $m_\pi \simeq 140$ MeV, and lattice results which are generally obtained at larger pion masses because of the simulation costs. Results of χPT typically contain so-called chiral logs. For instance, at one-loop order the prediction for the pion charge radius[18] reads

$$\langle r^2 \rangle_{\chi\mathrm{PT}}^{\mathrm{one-loop}} = c_1 + c_2 \log m_\pi^2 \tag{14}$$

with c_1 and c_2 being constants. A fit of our data based on this form is shown in Fig. 7. Chiral perturbation theory has also been applied to quenched QCD (qχPT). Here, at one loop the prediction for the charge radius is a constant. However, it is expected that in next order this is going to be modified[19]. At our mass values presumably the numerically most important contribution[20] consists of a term linear in m_π^2. Finally, in Fig. 7 we have also considered the vector meson dominance ansatz by parametrizing m_V in Eq. 11 as $m_V = a + b m_\pi^2$ which describes the data quite well.

5 Conclusion and Outlook

We have presented here the first calculation of the electromagnetic form factor of the pion based on an $\mathcal{O}(a)$ improved action and the concomitant improved vector current. This is seen to lead to significant changes in the prediction for the internal structure of the pion. Furthermore, the mass of the pion we reach in our calculations is considerably closer to the physical value than in previous work. We observe a decrease of the form factor for decreasing pion mass, which implies an increase of the RMS-radius. Such a mass-dependence of the radius is not seen in the Bethe-Salpeter approach. This highlights the importance of the gluons for the motion of the pion's center-of-mass which is neglected in the Bethe-Salpeter approach.

It has been predicted (and confirmed by lattice QCD calculations) that hadronic matter at a certain critical temperature will make a phase transition and deconfine. Quarks and gluons will then not be locked up anymore inside hadrons. One may expect that the internal structure of a given hadron changes as we approach this temperature. For instance, the binding of the quarks inside the pion could loosen, leading to a charge distributed over a larger space and to a changed form factor.

In order to study these questions, we have started to not only look at a free, isolated pion, but also at a pion immersed in a heat bath at a temperature $T \simeq 0.9\,T_c$, close to the critical temperature for the anticipated phase transition. In this case, on general grounds there are in principle three 'form factors'. Our first results indicate that the form factor reducing to $F(Q^2)$ at zero temperature shows no significant change so far. The analysis, however, needs to be refined and is currently the main subject of our ongoing project.

Acknowledgements

The authors thank R. Woloshyn and G. Colangelo for discussions. The work of J.v.d.H. and J.H.K. is part of the research program of the Foundation for Fundamental Research of Matter (FOM) and the National Organisation for Scientific Research (NWO). The research of E.L. is partly supported by Deutsche Forschungsgemeinschaft (DFG) under grant FOR 339/2-1. We thank the John von Neumann-Institut für Computing (NIC), Jülich, for the allocation of computer time for this project.

References

1. G. Martinelli and C.T. Sachrajda, Nucl. Phys. **B306** (1988) 865.
2. T. Draper, R.M. Woloshyn, W. Wilcox and K. Liu, Nucl. Phys. **B318** (1989) 319.
3. H.B. O'Connell, B.C. Pearce, A.W. Thomas and A.G. Williams, Prog. Part. Nucl. Phys. **39** (1997) 201.
4. J. van der Heide *et al.*, Phys. Lett. **B566** (2003) 131.
5. B. Sheikholeslami and R. Wohlert, Nucl. Phys. **B259** (1985) 572.
6. M. Lüscher *et al.*, Nucl. Phys. **B491** (1997) 323.
7. G. Martinelli, C.T. Sachrajda and A. Vladikas, Nucl. Phys. **B358** (1991) 212.
8. M. Lüscher, S. Sint, R. Sommer and H. Wittig, Nucl. Phys. **B491** (1997) 344.
9. M. Guagnelli and R. Sommer, Nucl. Phys. Proc. Suppl. **63** (1998) 886.
10. M.-C. Chu, M. Lissia and J.W. Negele, Nucl. Phys. **B360** (1991) 31.
11. M.W. Hecht and T.A. DeGrand, Phys. Rev. **D46** (1992) 2155.
12. R. Gupta, D. Daniel and J. Grandy, Phys. Rev. **D48** (1994) 3330.
13. P. Lacock *et al.*, Phys. Rev. **D51** (1995) 6403.
14. E. Laermann and P. Schmidt, Eur. Phys. J **C20** (2001) 541.
15. R.G. Edwards, U.M. Heller and T.R. Klassen, Nucl. Phys. **B517** (1998) 377.
16. T. Bhattacharya, R. Gupta, W. Lee and S. Sharpe, Phys. Rev. **63** (2001) 074505.
17. UKQCD Collaboration (K.C. Bowler *et al.*), Phys. Rev. **D62** (2000) 054506.
18. J. Gasser and H. Leutwyler, Ann. Phys. (N.Y.) **158** (1984) 142.
19. G. Colangelo and E. Pallante, Nucl. Phys. **B520** (1998) 433.
20. G. Colangelo, private communication.